Bandwidth Enhancement of the Resonant Cavity Antenna by Using Two Dielectric Superstrates

Muhannad A. Al-Tarifi, *Student Member, IEEE*, Dimitris E. Anagnostou, *Senior Member, IEEE*, Anthony K. Amert, and Keith W. Whites, *Senior Member, IEEE*

***Abstract*—We propose a novel approach to enhance the bandwidth of the high directivity of the resonant cavity antenna (RCA) by applying two dielectric layers as superstrates. The approach is based on creating two cavities corresponding to two operating frequency bands that combine to form a single wide band of operation. The RCA design is discussed in a methodological manner to determine the thicknesses of the superstrates, the separation distance between them, and the separation distance to the ground plane. We show that the proposed technique is capable of enhancing the bandwidth from 9% of the single superstrate RCA to 17.9% of the two superstrate RCA, with only 0.1-dB reduction of the maximum directivity (17.5 dBi). The presented design method can be replicated for any RCA with any directivity level and type of primary feeding. The performance of the analytically designed antenna is validated by simulation using commercial numerical electromagnetics software.**

***Index Terms*—Cavity resonators, dielectric slabs, directive antennas, electromagnetic reflection, leaky wave antennas.**

I. Introduction

THE broadside directivity of a simple primary radiator with a ground plane can be greatly enhanced by placing a planar partially reflecting surface (PRS) in front [1]. With multiple reflections of the wave inside the formed 1-D cavity structure, maximum radiation at broadside direction (normal to the plane of the PRS and ground) occurs when the PRS reflectivity is maximized and the cavity (ground-to-PRS separation region) has a thickness that yields to in-phase transmitted wave portions [1]–[3]. Accordingly, the structure is named a resonant cavity antenna (RCA).

The resonance condition of the RCA for maximum broadside radiation has been investigated intensively in literature [4]–[12]. Specifically, in order to obtain an in-phase wave addition at the broadside direction, the sum of all phases introduced to the wave after travelling one time back and forth should be multiple of 2π. Accordingly, the cavity thickness $(t_{\rm c})$ required for maximum broadside radiation at the resonance frequency $f_{\rm r}$ can be formulated as [4]

$$t_{\rm c} = \frac{\lambda_r}{4\pi}(\angle\Gamma_{PRS} + \angle\Gamma_{GND}) + N\frac{\lambda_{\rm r}}{2} \tag{1}$$

where $\lambda_{\rm r}$ is the wavelength in the cavity at the resonance frequency $f{\rm r}$, N is an integer, and $\angle\Gamma_{\rm PRS}$ and $\angle\Gamma_{\rm GND}$ are the phases of reflection coefficients due to a uniform plane wave in the cavity impinging normally into the PRS and the ground, respectively.

Although the formula in (1) yields to maximum radiation at broadside direction, it does not exactly represent the resonance condition for maximum broadside *directivity*. This is because the directivity (at any specific angle) is a function of radiation at all angles, whereas the formula in (1) considers phases at the broadside direction only. However, this formula demonstrates a reliable and simple approximation of the RCA resonance condition. Moreover, it provides a useful insight into the radiation variation with frequency [12].

The traditional RCA consists of a dielectric superstrate with high permittivity as a PRS, and a perfect electric conductor (PEC) plane as a ground. The far-field radiation by this antenna has been reported by using many analytical methods, such as ray-tracing analysis [3], transmission line analogy [13], leaky-wave analysis [14], and electromagnetic band-gap analysis [15]. All analytical methods concluded that the superstrate should be quarter-wavelength thick and placed at half-wavelength distance from the PEC plane (i.e., cavity is half-wavelength thick). Moreover, the maximum directivity increases as the permittivity of the superstrate increases, whereas the bandwidth decreases. Consequently, the operational bandwidth becomes a very critical factor at high directivity levels [16]–[18].

Recently, bandwidth enhancement of the RCA has been the focus of many research groups [19]–[33]. One studied method is using tapered-size elements of the reflecting sheet to achieve a tapered-index PRS [19], [20]. This corresponds to spherical-to-planar wave-front transformation, which enables radiation in plane-wave form by a larger aperture than the RCA of a uniform-index PRS. Hence, both of the directivity and the bandwidth are enhanced.

Another well-known method to enhance the bandwidth of the RCA is to employ a PRS with a reflection phase that increases (or slowly decreases) with frequency [21]–[29]. Such phase behavior restores the resonance condition of maximum broadside radiation over a wider bandwidth. However, the design of a PRS with the required phase properties was accomplished by using simulation to optimize several parameters related to the unit-cell element of the PRS, such as length and width. When two parallel

Manuscript received June 25, 2012; revised October 24, 2012; accepted November 09, 2012. Date of publication February 06, 2013; date of current version April 03, 2013. This work was supported in part by the National Science Foundation (NSF) through an Integrative, Hybrid and Complex Systems program grant ECCS-0824034, in part by the NSF EPSCoR under Grant #EPS-0903804, in part by the State of South Dakota, and in part by the Department of Defense DARPA MTO Young Faculty Award #N66001-11-1-4145.

The authors are with the Department of Electrical and Computer Engineering, South Dakota School of Mines and Technology, Rapid City, SD 57701 USA (e-mail: muhannad.al-tarifi@mines.sdsmt.edu; danagn@ieee.org; anthony.amert@sdsmt.edu; keith.whites@sdsmt.edu).

Color versions of one or more of the figures in this paper are available online at http://ieeexplore.ieee.org.

Digital Object Identifier 10.1109/TAP.2012.2231931

reflecting sheets were used then the separation distance between the sheets was optimized as well.

Studies have also shown that an array of radiators combined with a cavity structure can enhance the directivity with minimal effect to the bandwidth [30]–[32]. This technique benefits from the unused area inside the cavity to achieve an efficient illumination of the field upon the PRS. The advantage is that the directivity is enhanced by using both of the array and the cavity, whereas the bandwidth remains limited by the cavity solely. In most cases, this technique can be combined with other bandwidth enhancement techniques of the single fed RCA.

Lastly, size reduction of the RCA itself has been demonstrated to extremely enhance the bandwidth [33].

In this paper, two dielectric superstrates are applied to enhance the bandwidth of the RCA. The traditional RCA utilizes one superstrate and contains one cavity bordered by the PEC plane and the superstrate. Hence, directivity enhancement occurs at a single narrow frequency band that corresponds to the resonance of that cavity. In this study, we propose a two superstrate RCA that contains two cavities corresponding to two resonances. If the resonances are adequately produced at nearby frequencies, the frequency bands corresponding to these resonances can combine to create a single band of approximately twice the bandwidth of the traditional RCA. This approach is analogous to the directivity enhancement by using multiple superstrates to produce a pair of leaky-waves in the RCA structure [34].

In comparison with the previous approaches that examine the similar structure [21]–[25], [27]–[29], the concept presented in this paper has two main novel aspects. First, we present a step-by-step and non-iterative method to calculate the structure variables needed to enhance the bandwidth. On the other hand, the previous approaches require an iterative study by simulation to produce an increasing reflection phase with frequency for the PRS consisting of both superstrates and the separation between them. Such iterative study is lengthy because many variables need to be optimized in the process of designing a PRS of the required phase behavior.

The second novel aspect of the concept presented here is that it provides a better understanding of the physical insight behind the improvement of bandwidth. In other words, each variable of the structure is comprehensively digested with regard to its influence into the overall antenna performance. Hence, the fine-tuning employed the end of the design process ($\pm 5\%$) is effectively guided. In fact, we will show that the increasing reflection phase with frequency of the PRS is an outcome that is inherently developed by the end of the design process. The previous approaches, however, showed successful optimization of the PRS parameters to develop an increasing reflection phase, but the physical insight that explains this development has not yet been sufficiently investigated.

Initially, the antenna design proceeds from the traditional RCA to the two superstrate RCA in a simple systematic approach. The maximum directivity and operational bandwidth of the initially designed RCA are determined by simulation using the method of moments commercial numerical electromagnetic software IE3D by Zeland. Then, we investigate some chief parameters through simulation to demonstrate their effects on the antenna functionality and also to fine-tune the performance of the RCA. Next, we discuss the profile of the antenna, analogy to other enhanced-bandwidth RCAs, and generality of the design method. Lastly, a practical design situation is considered to validate the suitability of the presented approach to enhance the bandwidth in realistic perspectives.

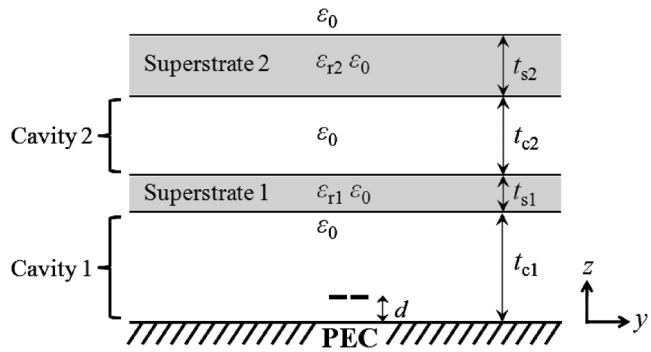

Fig. 1. General geometry of the two superstrate RCA structure.

II. Initial Design and Physical Principle

A general geometry of the two superstrate RCA is shown in Fig. 1. The structure consists of a PEC plane and two lossless, planar, homogeneous, and isotropic dielectric superstrate layers of relative permittivities ε_{r1} and ε_{r2}, and thicknesses t_{s1} and t_{s2}. The PEC and superstrates are parallel to each other and separated by free space regions (Cavity 1 and Cavity 2). Cavity 1, bordered by the PEC and Superstrate 1, has a thickness of t_{c1}, whereas Cavity 2, bordered by Superstrates 1 and 2, has thickness t_{c2}. A horizontal Hertzian dipole radiator (or feed) is placed in Cavity 1 at a distance d from the PEC. Ideally, the structure is assumed infinite in the $x-y$ plane.

The purpose of this section is to design all parameters (i.e., d, ε_{r1}, ε_{r2}, t_{s1}, t_{s2}, t_{c1}, and t_{c2}) to achieve high directivity at two nearby frequency bands, where each band corresponds to one cavity of the RCA. The bandwidth of operation will be determined based on the directivity values that are less than 3 dB below the maximum value.

We begin by designing the parameters related to the first cavity (d, ε_{r1}, t_{s1}, and t_{c1}) to produce the first band with a maximum directivity of 17.5 dBi. Then, the parameters related to the second cavity (ε_{r2}, t_{s2}, and t_{c2}) are designed to produce the second band with directivity values within a 3 dB range of 17.5 dBi. The second band will be designed adjacent to the first band so that the two bands combine together and create a single wider band.

We employ a mathematical code and a simulation tool in the design process. Particularly, we apply Chew's recursive formulas for a uniform plane wave scattering by a 1-D inhomogeneous dielectric media [35] to calculate the exact reflection coefficients observed by the cavity under examination. Based on these coefficients and the proposed conceptual design procedure, initial values of all antenna parameters are found. Afterwards, the antenna performance of the initial design is examined by simulation.

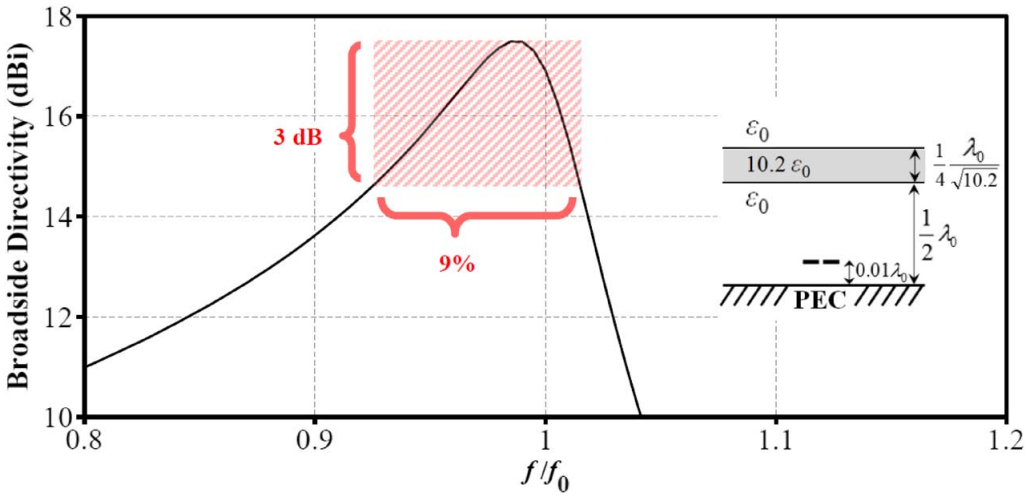

Fig. 2. Simulated broadside directivity versus frequency of the field radiated from the traditional RCA (the first cavity alone).

A. Design of the First Cavity

We design this cavity to obtain a resonance at the design frequency f_0 (i.e., $f_{r1} = f_0$) by following the conventional design rules of the traditional single superstrate RCA [13]. This implies that the cavity thickness (t_{c1}) is half a wavelength and the superstrate thickness (t_{s1}) is quarter a wavelength. For maximal directivity of the primary radiator, the Hertzian dipole is located very close to the PEC plane [36] at a hundredth-wavelength distance (i.e., $d = \lambda_0/100$). Last, a maximum directivity of 17.5 dBi is achieved by setting the superstrate relative permittivity (ε_{r1}) equal to 10.2.

It should be mentioned that in a realistic antenna, both the directivity and return loss should be considered for a complete performance evaluation. For this purpose, the absolute gain, which is a combination of directivity and return loss, will be used to evaluate the antenna performance of a practical example in Section IV-D. However, the focus of the current discussion is to enhance the bandwidth of high-directivity radiation (i.e., the pattern bandwidth), and this is why only the directivity is being considered in the investigation of the radiation performance of the whole cavity and also in determining the location of the Hertzian dipole radiator.

Fig. 2 shows the broadside directivity versus frequency of the radiated field from the first cavity. The maximum broadside directivity is 17.49 dBi (at $0.99f_0$) and the 3-dB bandwidth is 9% ($0.925f_0$–$1.015f_0$). We will refer to the aforementioned performance by the traditional RCA (first cavity alone) to evaluate the performance of the enhanced-bandwidth two superstrate RCAs to be designed in the next sections.

B. Physical Concept and Design of the Second Cavity

When a second superstrate is placed in front of the designed first cavity, a second cavity is formed (see Fig. 1). The wave radiated out of the first cavity encounters that second cavity, which affects the overall radiation of the RCA as a whole. Accordingly, the first cavity can be considered as the primary feed of the second cavity.

The first objective is to maintain the high directivity performance obtained from the first cavity in the frequency band from $0.925f_0$ to $1.015f_0$. In other words, the performance of the first cavity should not be affected by inserting the second superstrate in front. Hence, the second superstrate should have low reflection magnitude in this band. This can be achieved by setting the second superstrate thickness t_{s2} to be an integer multiple of half wavelengths [37] at the frequency of maximum directivity by the first cavity $(0.99f_0)$. For lowest superstrate thickness, the integer is set to unity, and t_{s2} is calculated as

$$t_{s2} = 0.5\frac{\left(\frac{\lambda_0}{0.99}\right)}{\sqrt{\varepsilon_{r2}}} = 0.505\frac{\lambda_0}{\sqrt{\varepsilon_{r2}}}. \tag{2}$$

This step is essential to continue the design, but its outcome is not necessarily the final (fine-tuned) value. Performing a fine tuning of t_{s2} after completing the initial design can be beneficial as to be discussed in Section III.

The second objective is to design the remaining parameters of the second cavity (ε_{r2} and t_{c2}) to enhance the directivity at an adjacent band ($0.835f_0$–$0.925f_0$). This requires both a sufficiently high reflection magnitude of the second superstrate [1], and also a cavity thickness t_{c2} properly designed to produce resonance in this band.

Fig. 3 shows the reflection magnitude of the second superstrate for different values of ε_{r2}. As ε_{r2} increases, the reflection magnitude increases in the band from $0.835f_0$ to $0.925f_0$. We require a reflection magnitude that is sufficient to increase the directivity level in this band to be within a 3 dB difference from the maximum directivity (>14.49 dBi). From Fig. 2, it is noticed that the directivity of the radiated wave from the first cavity varies from 11.76–14.49 dBi, which concludes that only 2.73 dB enhancement of the directivity is required by the effect of the second cavity. Accordingly, a relative permittivity ε_{r2} equal to 10.2 is initially selected. The effect of higher and lower values of ε_{r2} will be discussed in Section III.

Lastly, the cavity thickness t_{c2} is to be designed to enforce resonance of the second cavity in the band from $0.835f_0$ to $0.925f_0$. The entire structure of the first cavity (PEC, Cavity 1, and Superstrate 1) is recognized as the ground of the second cavity, whereas the second superstrate is recognized as the PRS.

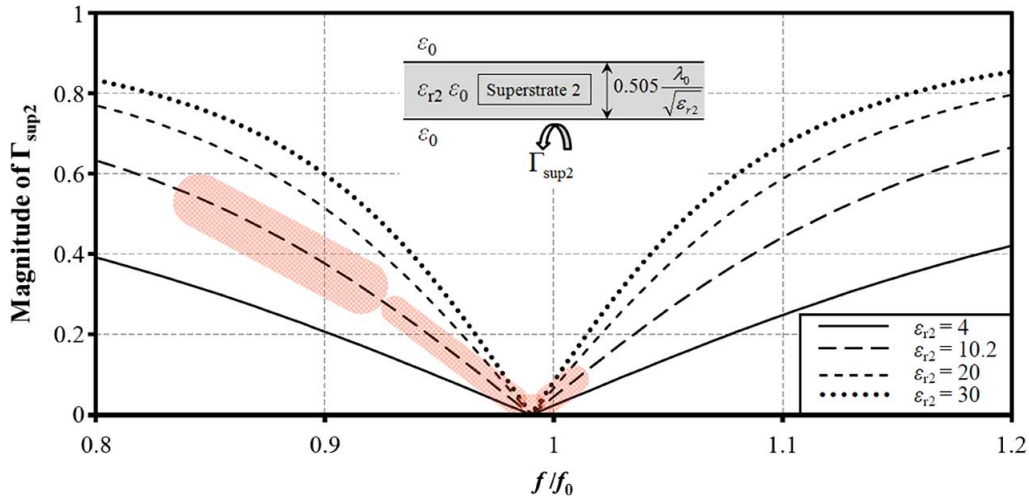

Fig. 3. Calculated magnitude of reflection coefficient versus frequency for a uniform plane wave impinging normally into the second superstrate with different values of its relative permittivity ε_{r2}. For $\varepsilon_{r2} = 10.2$, reflection magnitude is minimized at the bandwidth of the first cavity (thin shading) but has satisfactory levels at the bandwidth of the second cavity (wide shading).

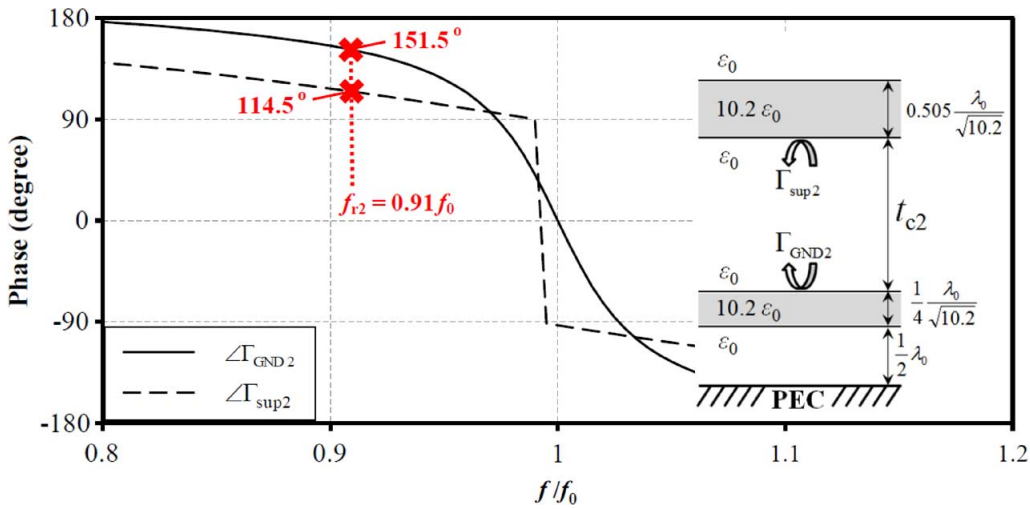

Fig. 4. Calculated phase of reflection coefficient versus frequency for a uniform plane wave inside Cavity 2, impinging normally into the ground (the whole first cavity) and the PRS (second superstrate).

By referring to the reflection phase plots of the ground and the PRS in Fig. 4, t_{c2} can be calculated by using (1) as

$$t_{c2} = \frac{\frac{\lambda_0}{0.91}}{4\pi}(151.5^\circ + 114.5^\circ) \times \frac{\pi}{180^\circ} = 0.406\lambda_0 \qquad (3)$$

where the resonance frequency f_{r2} is chosen to be equal to $0.91f_0$, and $N = 0$. This value of f_{r2} is initially chosen based on a careful observation of the band provided by the first cavity. The purpose is to create a second band that combines with first band before crossing the 3-dB limit (according to the definition of bandwidth). This is more likely to occur if the difference between the first and second resonances does not exceed the bandwidth provided by the first cavity ($BW_1 = 9\%$). Hence, $f_{r2} = (1 - 0.09)\ f_{r1}$ is selected (where $f_{r1} = f_0$). However, it is beneficial to vary f_{r2} slightly to fine-tune the bandwidth, which will be discussed in Section III.

C. Antenna Performance

The initial design of the second cavity, and the entire two superstrate RCA, is now complete. The antenna structure and broadside directivity are shown in Fig. 5. The maximum directivity is 17.4 dBi (at $0.99f_0$) and the 3-dB bandwidth is 17% ($0.845f_0$–$1.015f_0$). This bandwidth is more than 88% larger than that of the traditional RCA of a single superstrate (first cavity alone) shown in Fig. 2. The two-resonance behavior of the two superstrate RCA can be clearly observed from the directivity curve, where the upper part corresponds to the resonance of the first cavity and the lower part corresponds to the resonance of the second cavity. The resonances become more noticeable as ε_{r2} and f_{r2} vary, which will be discussed in the next section.

Fig. 6 shows the E- and H-plane radiation patterns of the designed two superstrate RCA at the edge and center frequencies of its operational band. The beam splitting appearance at the upper edge frequency $(1.015f_0)$ is similar to the pattern behavior of the traditional RCA [3]. This similarity is expected

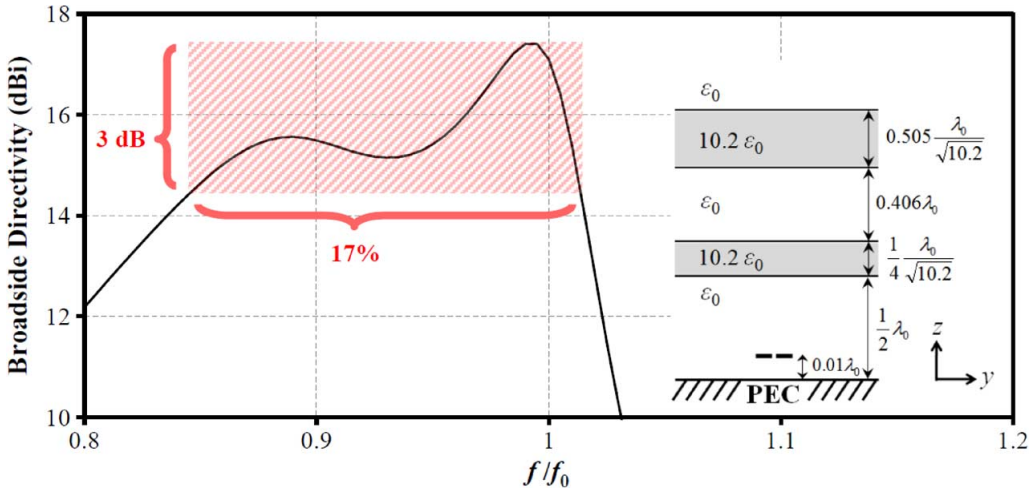

Fig. 5. Simulated broadside directivity versus frequency of the entire field radiated from the designed two superstrate RCA. The obtained 3-dB bandwidth is about 88% larger than that of the traditional RCA in Fig. 2.

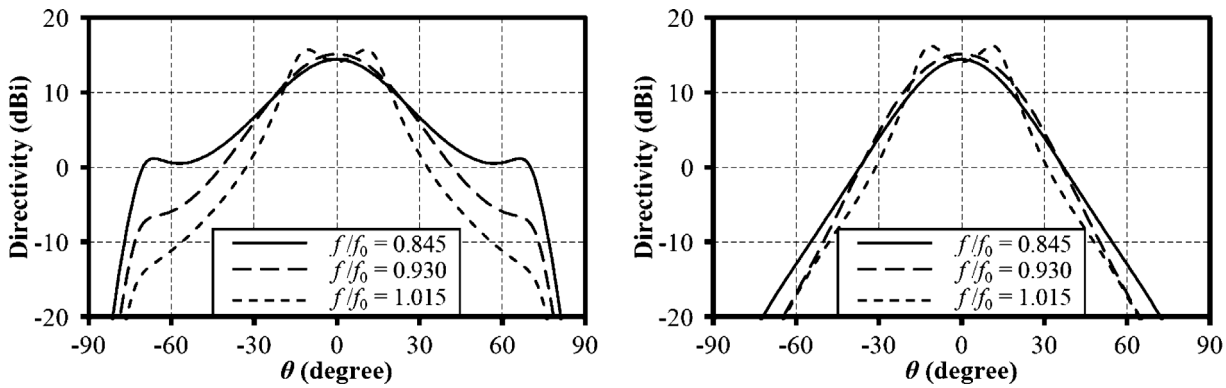

Fig. 6. Simulated E-plane (left) and H-plane (right) radiation patterns at the edge and center frequencies of the designed two superstrate RCA in Fig. 5.

because the first cavity of the two superstrate RCA, which corresponds to the upper resonance, is designed by following the conventional design rules of the traditional RCA.

III. Tuning of the Initial Design

A. Tuning of the Second Superstrate Thickness

The thickness of the second superstrate t_{s2} was the first determined parameter in the design process of the second cavity as presented in the preceding section. The initial design of the two superstrate RCA has an 88% enhanced bandwidth compared to that of the traditional RCA. Concurrently, the maximum directivity was minimally reduced (less than 0.1 dB). In this part, we perform a fine tuning of t_{s2} and discuss its effect on the broadside radiation of the RCA. For each value of t_{s2}, the thickness of Cavity 2 t_{c2} will be calculated by using (1) assuming a second resonance f_{r2} equal to $0.91 f_0$.

Fig. 7 shows the broadside directivity versus frequency for a varying t_{s2} from 0.46 to 0.52 of a wavelength. Table I lists the PRS and ground reflection phases as seen by Cavity 2, the calculated cavity thickness t_{c2}, and the bandwidth of the designed two superstrate RCA for each value of t_{s2}. It is found that as t_{s2} increases, the directivity decreases in the lower band and increases in the upper band. Such behavior agrees with our presented approach of the two superstrate RCA functionality. We refer to the curve of reflection magnitude shown in Fig. 3 for a second superstrate with relative permittivity ε_{r2} equal to 10.2 and thickness t_{s2} equal to 0.505 of a wavelength. As t_{s2} increases, the curve in Fig. 3 shifts to lower frequencies, which decreases the reflection magnitude of the second superstrate at the lower band (from $0.835 f_0$ to $0.925 f_0$) and, hence, the directivity at that band. Consistently, the shift of the reflection magnitude curve affects the directivity at the upper band as well. However, the nature of this effect relates jointly to the change in reflection magnitude and in the reflection phase of the second superstrate. Accordingly, it is difficult to predict that the directivity at the upper band increases as t_{s2} increases, as shown in Fig. 7, without performing the investigation by simulation.

From Fig. 7 and Table I, it can be seen that the bandwidth of the two superstrate RCA is better enhanced by the performed fine tuning of t_{s2}. For example, when t_{s2} is equal to 0.475 of a wavelength, a bandwidth equal to 19.7% and a maximum broadside directivity equal to 16.7 dBi are achieved. This is 119% enhanced bandwidth compared to that of the traditional RCA, with only 0.8 dB reduction of the maximum directivity.

B. Tuning of the Second Resonance Frequency

In the design process presented in the previous section, the thickness of Cavity 2 t_{c2} was the last determined parameter of the two superstrate RCA structure by using (1). This parameter was designed to provide a resonance suitable to enhance the directivity of the field radiated from the first cavity at the band

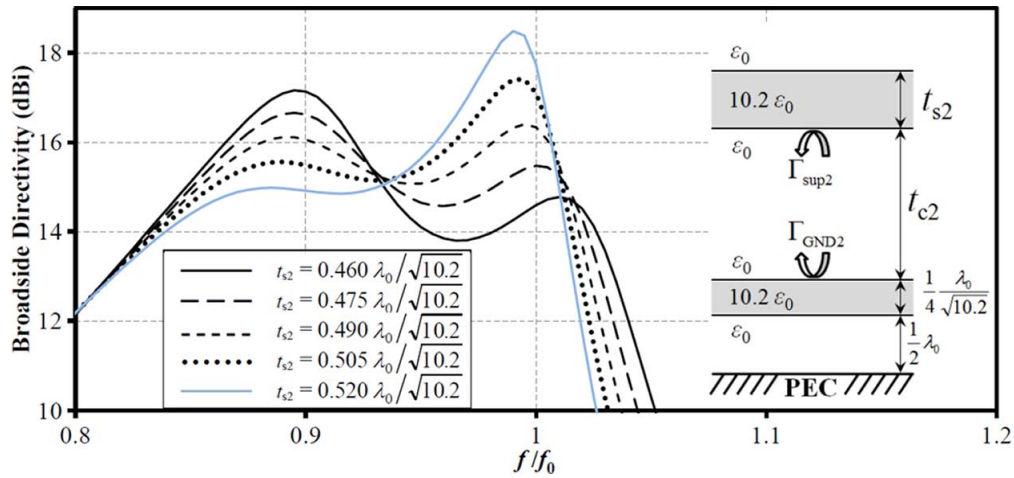

Fig. 7. Simulated broadside directivity versus frequency of the two superstrate RCA as the second superstrate thickness t_{s2} is varied from 0.46 to 0.52 wavelengths. The second superstrate resonance f_{r2} is assumed equal to $0.91f_0$. As t_{s2} increases, the directivity at the lower band decreases and at the upper band increases.

TABLE I
PRS AND GROUND REFLECTION PHASES (AS SEEN BY CAVITY 2), CALCULATED t_{c2}, AND BANDWIDTH OF THE DESIGNED TWO SUPERSTRATE RCA OF FIG. 7 FOR A VARIED t_{s2}. ($f_{r2} = 0.91f_0$ IS ASSUMED)

t_{s2}	$\angle\Gamma_{sup2}$	$\angle\Gamma_{GND2}$	t_{c2}	3-dB Bandwidth
$0.460\,\lambda_0/\sqrt{10.2}$	134.5^o	151.5^o	$0.437\,\lambda_0$	11.3%
$0.475\,\lambda_0/\sqrt{10.2}$	128.5^o	151.5^o	$0.427\,\lambda_0$	19.7%
$0.490\,\lambda_0/\sqrt{10.2}$	121.8^o	151.5^o	$0.417\,\lambda_0$	19.7%
$0.505\,\lambda_0/\sqrt{10.2}$	114.5^o	151.5^o	$0.406\,\lambda_0$	17%
$0.520\,\lambda_0/\sqrt{10.2}$	106.6^o	151.5^o	$0.394\,\lambda_0$	6.1%

adjacent to the lower edge of the band of the first cavity alone (traditional RCA). Specifically, t_{c2} was calculated based on an initial assumption of the second resonance f_{r2} to be equal to $0.91f_0$. Although this assumption has successfully enhanced the bandwidth by 88% compared to that provided by the traditional RCA, it is possible to fine-tune this enhancement by varying the selection of f_{r2} slightly.

Fig. 8 shows the broadside directivity versus frequency for a varying f_{r2} from $0.89f_0$ to $0.93f_0$. Table II lists the PRS and ground reflection phases as seen by Cavity 2, the calculated cavity thickness t_{c2}, and the bandwidth of the designed two superstrate RCA for each value of f_{r2}.It is found that as f_{r2} decreases and becomes more apart from $f_{r1}(= f_0)$, the directivity curve tends to show two distinct bands than one combined wider band. Such behavior limits the advantage of combining the bands before the directivity becomes more than 3 dB below the maximum as appears when $f_{r2} < 0.90f_0$. Furthermore, the maximal bandwidth is achieved at $f_{r2} = 0.90f_0$ and is equal to 17.9% (99% larger than that of the traditional RCA).

It is also informative to notice that the antenna at the upper band is minimally affected by the variation of f_{r2}. This agrees with the presented approach based on creating two independent resonances of the cavities. That is, any change of resonance in the second cavity (which only affects t_{c2}) should not influence the performance due to the first cavity (upper band) as long as the second superstrate has low reflection magnitude at that band (i.e., t_{s2} is unchanged).

C. Effect of the Second Superstrate Permittivity

Fig. 9 shows the broadside directivity versus frequency as the relative permittivity of the second superstrate ε_{r2} varies from 4 to 30. The electrical thickness of the second superstrate is fixed at 0.505 of a wavelength, whereas the cavity thickness is calculated by using (1) assuming a second resonance f_{r2} equal to $0.91f_0$. Table III lists the PRS and ground reflection phases as seen by Cavity 2, the calculated cavity thickness t_{c2}, and the bandwidth of the designed two superstrate RCA for each ε_{r2} selection.

Several antenna aspects can be inferred from the investigation of ε_{r2}:

a) The upper band is minimally influenced by changing ε_{r2}. This is expected by the presented design approach because the electrical thickness of the second superstrate is unchanged (0.505 of a wavelength) and, accordingly, it has a minimum reflection magnitude over the upper band.
b) The directivity values over the lower band increase as ε_{r2} increases, which is also expected by the presented design method. By referring to the reflection magnitude curves in Fig. 3, higher ε_{r2} corresponds to higher reflection magnitude at the lower band and, hence, higher directivities.
c) A compromise between the required directivity level at the lower band and the bandwidth should be made. From Fig. 9, a higher directivity at the lower band is achieved as ε_{r2} increases. However, the lower band becomes more separated from the upper band, and the desired single wider band can fail if the directivity at the edge frequency between the two bands ($\sim 0.93f_0$) deteriorates below the 3-dB difference from the maximum directivity ($\sim$17.4 dBi). To resolve this issue, one choice is to increase f_{r2} so that the lower band moves up and combines with the upper band. The other choice is to avoid using very high

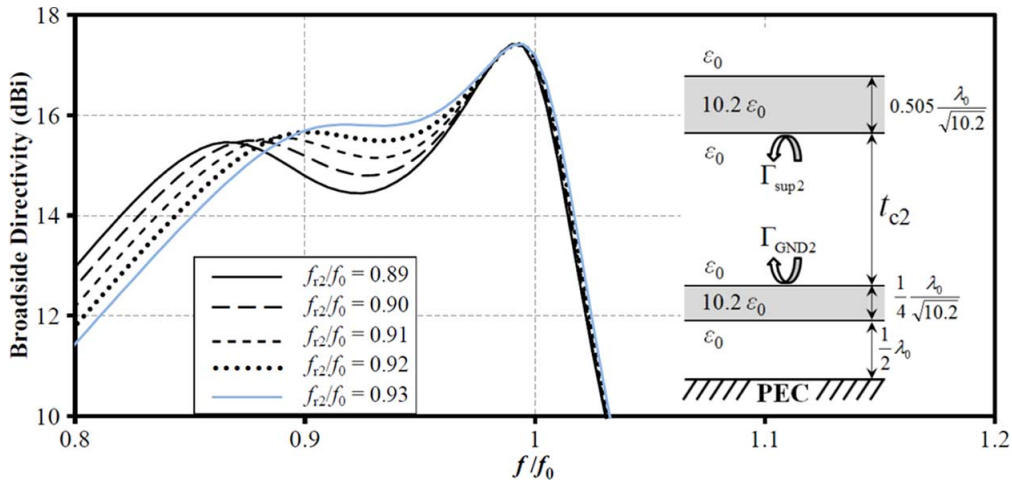

Fig. 8. Simulated broadside directivity versus frequency of the two superstrate RCA as the second resonance frequency f_{r2} is varied from $0.89f_0$ to $0.93f_0$. As f_{r2} increases, the lower band becomes more combined with the upper band.

TABLE II
PRS AND GROUND REFLECTION PHASES (AS SEEN BY CAVITY 2), CALCULATED t_{c2}, AND BANDWIDTH OF THE DESIGNED TWO SUPERSTRATE RCA OF FIG. 8 FOR A VARIED f_{r2}

f_{r2}	$\angle\Gamma_{sup2}$	$\angle\Gamma_{GND2}$	t_{c2}	3-dB Bandwidth
$0.89f_0$	120.0^o	158.6^o	$0.435\lambda_0$	9% (upper band)
$0.90f_0$	117.3^o	155.3^o	$0.421\lambda_0$	17.9%
$0.91f_0$	114.5^o	151.5^o	$0.406\lambda_0$	17%
$0.92f_0$	111.6^o	147.0^o	$0.390\lambda_0$	16.3%
$0.93f_0$	108.7^o	141.4^o	$0.374\lambda_0$	15.5%

values of ε_{r2} so that the second superstrate has a low reflection magnitude at the edge frequency between the bands ($\sim 0.93f_0$). However, this latter choice leads to lowered directivity at the lower band and prevents from achieving a much larger bandwidth if ε_{r2} is very low (see $\varepsilon_{r2} = 4$ in Fig. 9 and Table III).

IV. DISCUSSION AND GENERALIZATION

A. Antenna Profile

The main drawback of the presented enhanced-bandwidth two superstrate RCA is its increased profile. For example, the total z-direction profile of the designed two superstrate antenna in Fig. 5 is equal to $1.14\lambda_0$, which is 97% larger than the profile of the traditional single superstrate RCA of Fig. 2 ($0.58\lambda_0$). Such disadvantage is more likely to be a reasonable tradeoff to enhance the high-directivity bandwidth of the traditional RCA by simply placing a second superstrate in front. This can be much more efficient than using an array of primary radiators in a single superstrate RCA. More specifically, the presented technique is capable of enhancing the bandwidth for an existing traditional RCA with no need to modify its primary feeding or first superstrate.

B. Increasing Phase With Frequency

In this part, the analogy between the designed two superstrate RCA and the increasing reflection phase with frequency of the PRS is investigated. Specifically, we examine the designed structure to be comprised of a single ground plane (PEC), a single cavity (Cavity 1), and a single PRS plane (Superstrate 1, Cavity 2, Superstrate 2). The analysis of the structure from this prospective should be in agreement with the well-known reflection phase explanation of bandwidth enhancement [21]. That is, the reflection phase of the PRS increases with frequency to compensate for the naturally decreasing total phase that is the original reason for the narrow bandwidth of the traditional RCA. Consequently, the obtained total phase restores the resonant condition for maximum broadside radiation over a wider bandwidth.

Fig. 10 shows the calculated reflection phase versus frequency for the PRS, consisting of Superstrate 1, second cavity, and second superstrate, of the designed enhanced-bandwidth two superstrate RCA (shown in the inset). The phase increases with frequency indeed. This confirms the compliance between the two-resonance explanation (this paper) and the increasing phase explanation (Fig. 10) of the enhanced-bandwidth two superstrate RCA.

Here, it should be emphasized that the two-resonance explanation is a systematic design method that has no iterative steps. On the contrary, the increasing phase explanation is an outcome that is predicted to develop and is not effective as a design tool. To the best of our knowledge, before this paper, the only approach in literature to produce the wanted phase behavior was to perform a lengthy and iterative study of the PRS parameters.

C. Generalized Design Algorithm and Summary

Thus far, we have presented an example of bandwidth enhancement of the traditional single superstrate RCA by placing another superstrate of specific thickness and permittivity, at a specific separation distance in front of the antenna. The enhancement was demonstrated for a 17.5-dBi directivity antenna with no specific antenna features and, therefore, can be generalized as a proper method to enhance the bandwidth of the RCA of any directivity level. Furthermore, the presented approach is

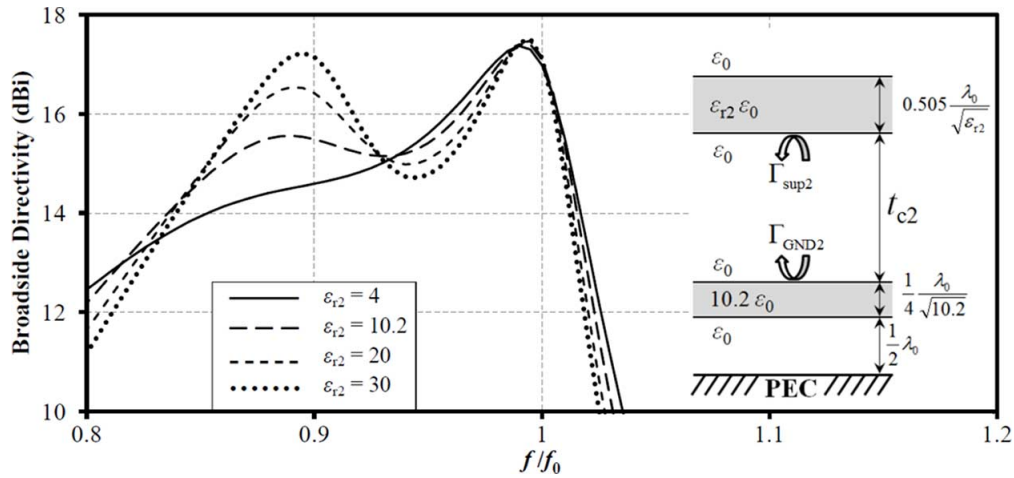

Fig. 9. Simulated broadside directivity versus frequency of the two superstrate RCA as the relative permittivity of the second superstrate ε_{r2} is varied from 4 to 30. The second superstrate resonance f_{r2} is assumed equal to $0.91f_0$. As ε_{r2} increases, the directivity at the lower band increases, but the directivity at the edge between the bands decreases.

TABLE III
PRS AND GROUND REFLECTION PHASES (AS SEEN BY CAVITY 2), CALCULATED t_{c2}, AND BANDWIDTH OF THE DESIGNED TWO SUPERSTRATE RCA OF FIG. 9 FOR A VARIED ε_{r2}. ($f_{r2} = 0.91f_0$ IS ASSUMED)

ε_{r2}	$\angle\Gamma_{sup2}$	$\angle\Gamma_{GND2}$	t_{c2}	3-dB Bandwidth
4	108.0^o	151.5^o	$0.396\,\lambda_0$	13.5%
10.2	114.5^o	151.5^o	$0.406\,\lambda_0$	17%
20	121.4^o	151.5^o	$0.417\,\lambda_0$	17%
30	126.3^o	151.5^o	$0.424\,\lambda_0$	17%

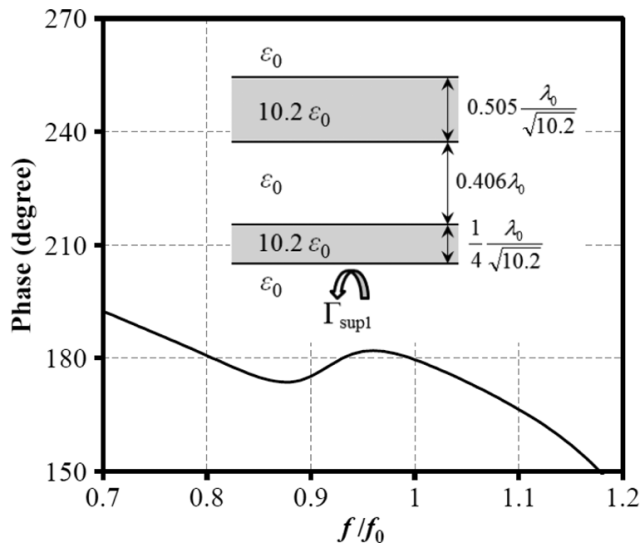

Fig. 10. Calculated phase of reflection coefficient ($\angle\Gamma_{sup1}$) versus frequency for a uniform plane wave inside Cavity 1, impinging normally into the PRS consisting of Superstrate 1, second superstrate, and the separation region between them. Notice that the phase increases with frequency over about 9% band, which compensates for the naturally decreasing total phase that is the original reason for the narrow bandwidth of the traditional RCA.

independent of the primary radiator in the first cavity. In fact, the physical principle for enhancement is based on the creation of a second resonance by designing a second cavity in front of a pre-designed first cavity. Consequently, the approach can also be applied to enhance the bandwidth of the RCA with any primary feeding (inside Cavity 1). In what follows, we summarize the design steps.

The design of an enhanced-bandwidth two superstrate RCA proceeds from a traditional single superstrate RCA by placing a dielectric layer (second superstrate) in front. The objective is to properly design all parameters associated with the addition of the second superstrate, including its thickness (t_{s2}), permittivity (ε_{r2}), and separation from the first superstrate (t_{c2}). We conclude from the investigations reported in the previous sections that designing a two superstrate RCA, with more than 50% enhanced bandwidth compared to that of the traditional RCA and less than 1-dB reduction of maximum directivity, can be accomplished in four non-iterative steps.

First, the permittivity of the second superstrate is assumed equal to that of the first superstrate (i.e., $\varepsilon_{r2} = \varepsilon_{r1}$). The validity of this assumption comes from the fact that the reflection magnitude from the second superstrate is higher for higher ε_{r2}, which is required in more directive traditional RCAs employing higher ε_{r1}.

Second, the thickness of the second superstrate (t_{s2}) is set equal to an integer multiple of half a wavelength at the frequency of maximum directivity provided by the first cavity alone. This setting insures a low reflection magnitude of the second superstrate at the high directivity band of the first cavity, which maintains this band for the whole RCA.

Third, the separation between the superstrates t_{c2} is to be calculated by using (1) to produce resonance in the second cavity at a frequency f_{r2} not much lower than that of the first cavity f_{r1}. In particular, it is conceptually appropriate to set f_{r2} lower than f_{r1} by the bandwidth of the first cavity alone. Consequently, the second cavity would develop a high directivity band (lower band) adjacent to that provided by the first cavity (upper band). The initial design of the enhanced-bandwidth RCA is now complete.

Last, the performance of the antenna can be fine-tuned through slight adjustments of t_{s2} and t_{c2}. More specifically, it is sufficient to vary these parameters only by $\pm 5\%$ of their initial

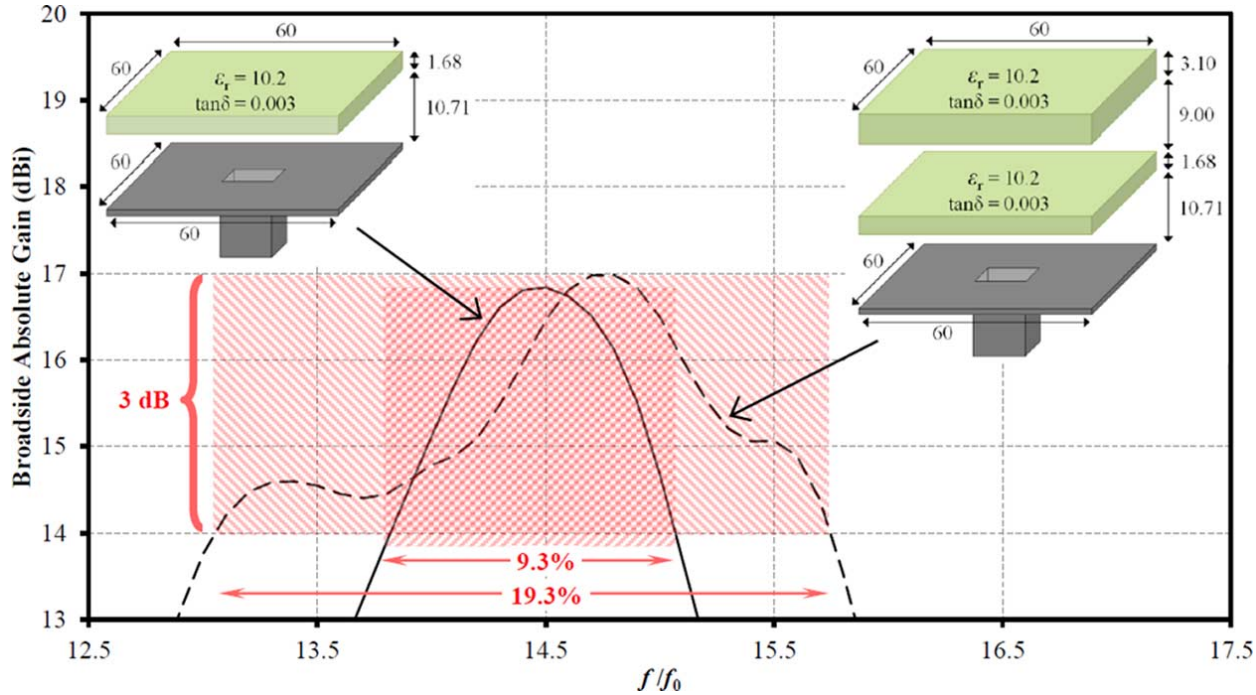

Fig. 11. Simulated broadside absolute gain versus frequency of the traditional RCA (top left) and the fine-tuned enhanced-bandwidth RCA (top right) based on a design frequency $f_0 = 14$ GHz. A practical situation is considered: the primary radiator is a Ku-band waveguide aperture, the ground is aluminum plate, the superstrates are lossy, the background is air, and the ground and superstrates are squares of finite sizes. All dimensions on structures are in millimeter.

values that were calculated in the second and third steps above. Moreover, it would be more efficient to vary these parameters with suitable background knowledge of their effects on the performance of the antenna as discussed in Section III.

D. Practical Example

In this part, we apply the presented bandwidth enhancement technique into a realizable RCA structure. That is, the primary radiator is a standard Ku-band waveguide (WR-62) aperture (instead of a Hertzian dipole), the ground plane is a finite-size aluminum plate (instead of an infinite PEC plane), the superstrates are finite-size lossy dielectric slabs (instead of infinite lossless slabs), and the background space is air (instead of free space). The purpose of this study is to verify that the presented bandwidth enhancement technique is valid for practical situations. *CST Microwave Studio 2011* is used to examine the performance of the designed RCAs.

With a design frequency $f_0(= f_{r1})$ equal to 14 GHz ($\lambda_0 = 21.42$ mm), the traditional RCA is initially constructed as illustrated in the inset of Fig. 11 (top left). The absolute gain at broadside shows a maximum gain of 16.84 dBi at 14.5 GHz, and a 3-dB bandwidth of 9.3%.

Based on the performance of the traditional RCA and by following the bandwidth enhancement technique presented in Section II, a second superstrate of 3.24 mm thickness (half-wavelength at 14.5 GHz) is placed at 9.13 mm distance above the first superstrate [$f_{r2} = 12.7$ GHz is applied in (1)]. The absolute gain of the resulted structure (not shown here) exhibits only a 21.5% enhancement of bandwidth compared to that of the traditional RCA, with 0.2 dB increase of the maximum gain value.

As the last step, the second superstrate thickness and its separation from the first superstrate are fine-tuned within $\pm 5\%$ of their initial calculated values (3.24 and 9.13 mm, respectively). Fig. 11 shows the fine-tuned structure (top right) and its absolute gain at broadside. The maximum gain is 16.98 dBi at 14.75 GHz, and the 3-dB bandwidth is 19.3%. This bandwidth is 107% enhanced compared to that of the traditional RCA and, yet, the maximum gain is slightly increased (by 0.14 dB). Although the frequency of maximum gain is shifted from 14.5 to 14.75 GHz, probably due to some complications related to the finite size of the structure, the enhanced bandwidth outcome verifies the suitability of the technique presented in this paper when applied to practical RCA structures.

V. Conclusion

A novel technique to enhance the bandwidth of the RCA by using two dielectric superstrates was presented. The technique is based on creating two adjacent high directivity bands corresponding to the two cavities of the antenna. In a representative example, the design of the two superstrate RCA has advanced from a traditional RCA with a single superstrate by placing a second superstrate in front, where the parameters related to this addition were determined in a methodical and non-iterative manner. The bandwidth was approximately doubled whereas the maximum directivity was insignificantly affected. In general, the presented technique can be applied to enhance the bandwidth of any traditional RCA regardless its maximum directivity and type of primary feeding.

Acknowledgment

The authors would like to thank the anonymous reviewers for their useful and constructive comments that helped improve this manuscript.

REFERENCES

[1] G. V. Trentini, "Partially reflecting sheet arrays," *IRE Trans. Antennas Propag.*, vol. AP-4, no. 4, pp. 666–671, Oct. 1956.

[2] A. P. Feresidis and J. C. Vardaxoglou, "High gain planar antenna using optimised partially reflective surfaces," *Proc. Inst. Elect. Microw. Antennas Propag.*, vol. 148, no. 6, pp. 345–350, Dec. 2001.

[3] M. A. Al-Tarifi, D. E. Anagnostou, A. K. Amert, and K. W. Whites, "Bandwidth enhancement of the cavity resonance antenna (CRA) using multiple dielectric superstrate layers," presented at the 2011 IEEE MTT-S Int. Microwave Symp., Baltimore, MD, USA, June 5–10, 2011.

[4] A. P. Feresidis, G. Goussetis, S. Wang, and J. C. Vardaxoglou, "Artificial magnetic conductor surfaces and their application to low-profile high-gain planar antennas," *IEEE Trans. Antennas Propag.*, vol. 53, no. 1, pp. 209–215, Jan. 2005.

[5] A. R. Weily, T. S. Bird, and Y. J. Guo, "A reconfigurable high-gain partially reflecting surface antenna," *IEEE Trans. Antennas Propag.*, vol. 56, no. 11, pp. 3382–3390, Nov. 2008.

[6] L. Zhou, H. Li, Y. Qin, Z. Wei, and C. T. Chan, "Directive emissions from subwaveength metamaterial-based cavities," *Appl. Phys. Lett.*, vol. 86, p. 101101, Feb. 2005.

[7] F. Costa, E. Carrubba, A. Monorchio, and G. Manara, "Multi-frequency highly directive Fabry-Perot based antenna," presented at the 2008 IEEE AP-S Int. Symp., San Diego, CA, Jul. 5–11, 2008.

[8] L. Moustafa and B. Jecko, "Broadband high gain compact resonator antennas using combined FSS," presented at the 2008 IEEE AP-S Int. Symp., San Diego, CA, USA, July 5–11, 2008.

[9] S. A. Muhammad, R. Sauleau, and H. Legay, "Compact metallic self-polarizing Fabry-Perot cavity antennas with small lateral size," in *Proc. EuCAP '11*, Rome, Italy, April 11–15, 2011.

[10] Z. G. Liu, "Fabry-Perot resonator antenna," *J. Infrared Milli. Terahz. Waves*, vol. 31, no. 4, pp. 391–403, Dec. 2009.

[11] A. Ourir, A. de Lustrac, and J.-M. Lourtioz, "All-metamaterial-based subwavelength cavities ($\lambda/60$) for ultrathin directive antennas," *Appl. Phys. Lett.*, vol. 88, no. 8, pp. 84103-1–84103-3, Feb. 2006.

[12] J. R. Kelly, T. Kokkinos, and A. P. Feresidis, "Analysis and design of sub-wavelength resonant cavity type 2-D leaky-wave antennas," *IEEE Trans. Antennas Propag.*, vol. 56, no. 9, pp. 2817–2825, Sep. 2008.

[13] D. R. Jackson and N. G. Alexopoulos, "Gain enhancement methods for printed circuit antennas," *IEEE Trans. Antennas Propag.*, vol. 33, no. 9, pp. 976–987, Sep. 1985.

[14] D. R. Jackson and A. A. Oliner, "A leaky-wave analysis of the high-gain printed antenna configuration," *IEEE Trans. Antennas Propag.*, vol. 36, no. 7, pp. 905–910, Jul. 1988.

[15] C. Serier, C. Cheype, R. Chantalat, M. Thevenot, T. Monédière, A. Reineix, and B. Jecko, "1-D photonic bandgap resonator," *Microw. Opt. Technol. Lett.*, vol. 29, no. 5, pp. 312–315, Jun. 2001.

[16] G. Lovat, P. Burghignoli, and D. R. Jackson, "Fundamental properties and optimization of broadside radiation from uniform leaky-wave antennas," *IEEE Trans. Antennas Propag.*, vol. 54, no. 5, pp. 1442–1452, May 2006.

[17] G. Lovat, P. Burghignoli, F. Capolino, and D. R. Jackson, "Bandwidth analysis of highly-directive planar radiators based on partially-reflecting surfaces," in *Proc. EuCAP 2006*, Nice, France, Nov. 6–10, 2006.

[18] T. Zhao, D. R. Jackson, J. T. Williams, and A. A. Oliner, "Simple CAD model for a dielectric leaky-wave antenna," *IEEE Antennas Wireless Propag. Lett.*, vol. 3, no. 1, pp. 243–245, Dec. 2004.

[19] Z.-G. Liu, W.-X. Zhang, D.-L. Fu, Y.-Y. Gu, and Z.-C. Ge, "Broadband Fabry-Perot resonator printed antennas using FSS superstrate with dissimilar size," *Microw. Opt. Technol. Lett.*, vol. 50, no. 6, pp. 1623–1627, June 2008.

[20] Z.-G. Liu, R. Qiang, and Z.-X. Cao, "A novel broadband Fabry-Perot resonator antenna with gradient index metamaterial superstrate," presented at the 2010 IEEE AP-S Int. Symp., Toronto, ON, Canada, Jul. 11–17, 2010.

[21] A. P. Feresidis and J. C. Vardaxoglou, "A broadband high-gain resonant cavity antenna with single feed," in *Proc. EuCAP '06*, Nice, France, Nov. 6–10, 2006.

[22] T.-H. Vu, K. Mahdjoubi, A.-C. Tarot, and S. Collardey, "Bandwidth enlargement of planar EBG antennas," in *Proc. Conf. Loughborough Antennas Propag.*, Loughborough, U.K., Apr. 2007.

[23] L. Moustafa and B. Jecko, "EBG structure with wide defect band for broadband cavity antenna applications," *IEEE Antennas Wireless Propag. Lett.*, vol. 7, pp. 693–696, 2008.

[24] Y. Li and K. P. Esselle, "Consideration of bandwidth of the small EBG-resonator antenna using the in-phase highly-reflecting surfaces," presented at the 2009 IEEE AP-S Int. Symp., Charleston, SC, Jun. 1–5, 2009.

[25] C. Mateo-Segura, A. P. Feresidis, and G. Goussetis, "Analysis of broadband highly-directive Fabry-Perot cavity Leaky-Wave antennas with two periodic layers," presented at the 2010 IEEE AP-S Int. Symp., Toronto, ON, Jul. 11–17, 2010.

[26] M. Mirbach and W. Menzel, "A High gain planar antenna with improved bandwidth using a Fabry-Perot resonator," in *Proc. EuCAP '10*, Barcelona, Spain, Apr. 12–16, 2010.

[27] M. A. Al-Tarifi, D. E. Anagnostou, A. K. Amert, and K. W. Whites, "Multiple superstrates technique for a broadband cavity resonance antenna (CRA)," presented at the 2011 IEEE AP-S Int. Symp., Spokane, WA, USA, Jul. 3–8, 2011.

[28] Y. Ge, K. P. Esselle, and T. S. Bird, "The use of simple thin partially reflective surfaces with positive reflection phase gradients to design wideband, low-profile EBG resonator antennas," *IEEE Trans. Antennas Propag.*, vol. 60, no. 2, pp. 743–750, Feb. 2012.

[29] D. Kim, J. Ju, and J. Choi, "A mobile communication base station antenna using a genetic algorithm based Fabry-Perot resonance optimization," *IEEE Trans. Antennas Propag.*, vol. 60, no. 2, pp. 1053–1058, Feb. 2012.

[30] L. Leger, T. Monediere, and B. Jecko, "Enhancement of gain and radiation bandwidth for a planar 1-D EBG antenna," *IEEE Microw. Wireless Components Lett.*, vol. 15, no. 9, pp. 573–575, Sep. 2005.

[31] R. Gardelli, M. Albani, and F. Capolino, "Array thinning by using antennas in a Fabry-Perot cavity for gain enhancement," *IEEE Trans. Antennas Propag.*, vol. 54, no. 7, pp. 1979–1990, Jul. 2006.

[32] A. R. Weily, K. P. Esselle, T. S. Bird, and B. C. Sanders, "High gain antenna with improved radiation bandwidth using dual 1-D EBG resonators and array feed," presented at the 2006 IEEE AP-S Int. Symp., Albuquerque, NM, USA, Jul. 9–14, 2006.

[33] Y. J. Lee, J. Yeo, R. Mittra, and W. S. Park, "Applications of electromagnetic bandgap (EBG) superstrates with controllable defects for a class of patch antennas as spatial angular filters," *IEEE Trans. Antennas Propag.*, vol. 53, no. 1, pp. 224–235, Jan. 2005.

[34] D. R. Jackson and A. A. Oliner, "Leaky-wave propagation and radiation for a narrow-beam multiple-layer dielectric structure," *IEEE Trans. Antennas Propag.*, vol. 41, no. 3, pp. 344–348, Mar. 1993.

[35] W. C. Chew, *Waves and Fields in Inhomogeneous Media*. New York: Van Nostrand, 1990, pp. 49–53.

[36] C. A. Balanis, *Antenna Theory, Analysis and Design*, 3rd ed. New York, NY, USA: Wiley, 2005, pp. 197–205.

[37] C. A. Balanis, *Advanced Engineering Electromagnetics*. New York, NY, USA: Wiley, 1989, ch. 5, pp. 224–225.

Muhannad A. Al-Tarifi (S'08) received the B.S. degree in electrical engineering from the Jordan University of Science and Technology, Ar Ramtha, in 2005. He is currently working towards the Ph.D. degree in nanoengineering from the South Dakota School of Mines and Technology, Rapid City, SD, USA.

His research focuses on applications of artificial dielectric materials in antennas and microwave circuits.

Dimitris E. Anagnostou (S'98–M'05–SM'10) received the B.S.E.E. degree from the Democritus University of Thrace, Xanthi, Greece, in 2000 and the M.S.E.E. and Ph.D. degrees from the University of New Mexico, Albuquerque, NM, USA, in 2002 and 2005, respectively.

From 2005 to 2006, he was a Post-Doctoral Fellow at the Georgia Institute of Technology, Atlanta, GA, USA. Since 2007 he has been an Assistant Professor of Electrical and Computer Engineering at the South Dakota School of Mines and Technology, Rapid City, SD, USA. He has published 70 peer-reviewed journal and conference papers. His interests include reconfigurable, autonomous, flexible, electrically small and miniaturized antennas and arrays, analytical design methods for antennas and microwave components, metamaterial applications, direct-write, "green" and Paper RF electronics, applications of artificial dielectrics and dielectric superstrates, leaky-wave antennas, cavity resonance antennas, antennas on PV-cells, RF-MEMS, propagation in tunnels, and microwave packaging.

Dr. Anagnostou was the recipient of the 2011 DARPA Young Faculty Award and the 2010 IEEE Antennas and Propagation Society (AP-S) John Kraus Antenna Award. He also received the 2011 AFRL Summer Faculty Fellowship by the ASEE. In 2006, he was recognized as a distinguished scientist living abroad by the Hellenic Ministry of Defense. He holds one patent on reconfigurable antennas. He serves as Associate Editor for the IEEE TRANSACTIONS ON ANTENNAS AND PROPAGATION and the *Springer International Journal of Machine Learning and Cybernetics*, as a member of the TPC and session chair for *IEEE Antennas and Propagation International Symposia*, and as a reviewer for 14 international publications including IEEE TRANSACTIONS ON ANTENNAS AND PROPAGATION, TRANSACTIONS ON MICROWAVE THEORY AND TECHNIQUES, *AP-S Magazine*, *AWPL*, and *MWCL*. He has given two workshop presentations at *IEEE AP-S* and *IEEE MTT-S* International Symposia. Dr. Anagnostou is a member of Eta Kappa Nu, ASEE, and of the Technical Chamber of Greece.

Anthony K. Amert received the B.S. and M.S. degrees in electrical engineering from the South Dakota School of Mines and Technology, Rapid City, SD, USA, in 2004 and 2006, respectively.

Since 2006, he has been a Research Scientist at the South Dakota School of Mines and Technology working on the miniaturization of microwave devices. His research interests include the development and characterization of electromagnetic materials, the design and manufacturing of devices that can benefit from such materials, and device characterization.

Keith W. Whites received the B.S.E.E. degree from the South Dakota School of Mines and Technology, Rapid City, in 1986 and the M.S. and Ph.D. degrees from the University of Illinois at Urbana-Champaign, Urbana, IL, USA, in 1988 and 1991, respectively.

From 1991 to 2001, he was an Assistant and later an Associate Professor at the University of Kentucky in the Department of Electrical and Computer Engineering. Since 2001, he has been at the South Dakota School of Mines and Technology where he is currently Professor and Steven P. Miller Endowed Chair in Electrical Engineering teaching courses in applied electromagnetics and wireless communications, among other topics. His research interests include the analysis, design, and measurement of artificial electromagnetic materials; electromagnetic materials characterization; antenna miniaturization; high-impedance and textured surfaces; and direct-write fabrication of antennas and microwave frequency devices; among others. He has coauthored an electromagnetics textbook and is the author of more than 90 refereed journal and conference papers on various aspects of electromagnetics.

Dr. Whites is the 1999 recipient of the R.W.P. King Prize Paper Award from the IEEE Antennas and Propagation Society and recipient of NSF Faculty Early Career Development (CAREER) and Research Initiation Awards. He is a member of Tau Beta Pi and Eta Kappa Nu.